



Originally published as:

Floor, G. H., Queralt, I., Hidalgo, M., Marguí, E. (2015): Measurement uncertainty in Total Reflection X-ray Fluorescence. - *Spectrochimica Acta Part B: Atomic Spectroscopy*, 111, p. 30-37.

DOI: <http://doi.org/10.1016/j.sab.2015.06.015>

# 1 Measurement uncertainty in total reflection X- 2 ray fluorescence

3 G.H.Floor<sup>a,1</sup>, I.Queralt<sup>b</sup>, M.Hidalgo<sup>c</sup>, E.Marguí<sup>c</sup>

4 <sup>a</sup> GFZ German Research Centre for Geosciences Section 3.4. Earth Surface Geochemistry, Telegrafenberg,  
5 14473 Postdam, Germany

6 <sup>b</sup> Institute of Earth Sciences Jaume Almera ICTJA-CSIC. Solé Sabaris s/n, 08028 Barcelona, Spain

7 <sup>c</sup> Department of Chemistry. University of Girona. Campus Montilivi s/n, 17071-Girona, Spain

## 8 Abstract

9 Total reflection X-ray fluorescence (TXRF) spectrometry is a multi-elemental  
10 technique using micro-volumes of sample. This work assessed the components  
11 contributing to the combined uncertainty budget associated with TXRF measurements  
12 using Cu and Fe concentrations in different spiked and natural water samples as an  
13 example. The results showed that an uncertainty estimation based solely on the count  
14 statistics of the analyte is not a realistic estimation of the overall uncertainty, since  
15 the depositional repeatability and the relative sensitivity between the analyte and the  
16 internal standard are important contributions to the uncertainty budget. The  
17 uncertainty on the instrumental repeatability and sensitivity factor could be estimated  
18 and as such, potentially relatively straightforward implemented in the TXRF  
19 instrument software. However, the depositional repeatability varied significantly from  
20 sample to sample and between elemental ratios and the controlling factors are not  
21 well understood. By a lack of theoretical prediction of the depositional repeatability,  
22 the uncertainty budget can be based on repeat measurements using different  
23 reflectors. A simple approach to estimate the uncertainty was presented. The  
24 measurement procedure implemented and the uncertainty estimation processes  
25 developed were validated from the agreement with results obtained by inductively  
26 coupled plasma – optical emission spectrometry (ICP-OES) and/or  
27 reference/calculated values.

28 **Keywords:** TXRF, measurement uncertainty, data quality, method validation.

## 29 1. Introduction

30 Total reflection X-ray fluorescence spectrometry (TXRF) is a multi-elemental and  
31 micro-analytical technique. The TXRF technique is a variation of energy-dispersive

---

<sup>1</sup> Corresponding author: geerke.floor@gfz-potsdam.de

32 XRF where the primary beam strikes the sample at a very small incident angle  
33 ( $\approx 0.1^\circ$ ) leading to lower scattering and an improvement of detection limits. To  
34 perform analysis under total-reflection conditions, samples must be provided as thin  
35 films [1]. For liquid samples, this is done by depositing as little as 5–50  $\mu\text{L}$  of sample  
36 on a reflective carrier with a subsequent drying by applying heat or vacuum.  
37 Preparation of samples as thin layer exclude absorption and secondary excitation and  
38 thus, the quantification in TXRF analysis can be done simply by the addition of an  
39 internal standard to the sample prior to deposition [2-3].

40

41 Most of the published TXRF analyses in the last decades, were performed using large-  
42 scaled instruments with high-power X-ray tubes, demanding water-cooling systems  
43 and liquid-nitrogen cooled detectors. However, in recent years, the development and  
44 commercialization of benchtop TXRF instrumentation, which offer extreme simplicity  
45 of operation, in a low-cost compact design, have promoted its application in industry  
46 as well as in research activities for trace element analysis [4-6]. However, despite  
47 the efficiency and simplicity of the benchtop TXRF instrumentation, this technique is  
48 very little employed for environmental and geochemical analyses compared to other  
49 techniques, such as inductively coupled plasma - mass spectrometry or optical  
50 emission spectrometry (ICP-MS or ICP-OES) and Atomic Absorption Spectrometry  
51 (AAS).

52

53 To ensure the validation of the data interpretation in environmental analyses, the  
54 performance and 'fit-for-purpose' of the method should be demonstrated and  
55 sufficient information should be provided about the followed methodology [7-10].  
56 The international standard ISO/IEC 17025 states that the performance of a  
57 measurement procedure should be evaluated based on one or a combination of the  
58 following approaches: a) the use of reference materials, b) the comparison of results  
59 achieved with other methods, c) inter-laboratory comparison, d) systematic  
60 assessments of the factors influencing the result and e) the assessment of the  
61 uncertainty of the results [11]. Therefore, in this paper, we contribute to the  
62 validation of TXRF analyses by assessing the factors contributing to the measurement  
63 uncertainty. In previous works theoretical models have been combined with the  
64 empirical uncertainty based on repetitive measurements of standards [12, 13].  
65 However, the theoretical uncertainties and empirical model did not always give the  
66 same result. In this study, we want to present a mathematical model explaining the  
67 measurement procedure which can be applied in a practical way to samples. For that,  
68 an example of copper (Cu) and iron (Fe) in natural waters is used. Copper enters  
69 drinking water primarily through plumbing materials. Copper is highly toxic as it is

70 carcinogens and mutagens in nature [14-15]. Hence, the European Water Framework  
71 Directive (WFD) [16] and the guidelines of the World Health Organization (WHO)  
72 handle a maximum Cu concentration of  $2 \text{ mg}\cdot\text{L}^{-1}$ . Iron is an unaesthetic parameter in  
73 drinking water and therefore included in the WFD [16] as an indicator parameter at  
74  $0.2 \text{ mg}\cdot\text{L}^{-1}$ . Iron plays an important role in element cycling and therefore often  
75 studied within geochemical studies [17-18]. In this manuscript, the focus is on which  
76 factors, including the sample characteristics and the measurement protocol, influence  
77 the results and the uncertainty budget of Cu and Fe determinations by TXRF to  
78 provide an example how a realistic uncertainty can be estimated in TXRF  
79 measurements.

80

## 81 **2. Method and materials**

### 82 **2.1 Reagent, materials and samples**

83 Stock solutions of  $1000 \pm 0.5 \text{ mg}\cdot\text{kg}^{-1}$  (Spectroscan, TECKNOLAB A/S, Norway) of  
84 Cu, Fe, Rh and Y were used to prepare standard solutions and spiked samples. High  
85 purity water used for dilution of stock solutions was obtained from a Milli-Q purifier  
86 system operated at  $18 \text{ M}\Omega\cdot\text{cm}$  (Millipore Corp., Bedford, MA).

87 Several water samples with different matrices have been used for analyses: the  
88 certified reference material SPS-WW2 ("Reference Material for Measurement of  
89 Elements in Wastewaters", Spectrapure Standard, Manglerud, Oslo, Norway), spiked  
90 tap/river water samples at the level of around  $2 \text{ mg}\cdot\text{kg}^{-1}$  of Cu and  $4 \text{ mg}\cdot\text{kg}^{-1}$  of Fe, a  
91 municipal waste water sample and a mine water sample. All samples (except the  
92 certified reference material) were filtered through a  $0.45 \mu\text{m}$  cellulose acetate filter  
93 (Millipore) before TXRF analysis.

94 In TXRF analysis, the sample carrier plays an important role with regard to the  
95 achievement of optimal analytical results. In this work, taking into account the higher  
96 resistance and the lower background, quartz glass discs (Bruker AXS Microanalysis  
97 GmH, Berlin, Germany) with a diameter of 30 mm and a thickness of  $3 \pm 0.1 \text{ mm}$  were  
98 used as sample holders for introducing the sample into the TXRF equipment.

99

### 100 **2.2 Instrumentation**

101 TXRF analysis of standards and samples was performed with the benchtop S2  
102 PICOFOX™ spectrometer (Bruker AXS Microanalysis GmbH, Berlin, Germany). The  
103 spectrometer specifications and operating conditions used are summarized in Table  
104 1. One of the advantages of this spectrometer compared to other existing systems is

105 that is equipped with an air-cooled low-power X-ray tube and a Peltier cooled silicon  
106 drift detector and thus, no cooling media and gas consumption are required. As it is  
107 shown in Table 1, the anode of the X-ray tube in the TXRF instrument is made of W.  
108 This fact allows performing TXRF analysis using K-lines of high atomic number  
109 elements such as Sn and Cd (in conventional Mo-based X-ray tubes less intense L-  
110 lines have to be used for this purpose) and thus the limits of detection for heavy  
111 elements are improved. However, limits of detection for the 4<sup>th</sup> period elements  
112 (Z=19-36) are higher than those associated with Mo anode X-ray tubes (between 1  
113 and 10  $\mu\text{g}\cdot\text{kg}^{-1}$ ). Limits of detection calculated for the determination of Cu and Fe  
114 using the operating conditions displayed in Table 1 were around 30 and 40  $\mu\text{g}\cdot\text{kg}^{-1}$ ,  
115 respectively.

116 For comparison, the samples were also analyzed by using an ICP-OES spectrometer  
117 Varian Liberty (Springvale, Australia) with a V-groove nebulizer of which the  
118 instrumental parameters and measurement conditions are also shown in Table 1.

### 119 **2.3 TXRF measurements**

120 Samples and standard solutions were prepared as following for TXRF analysis: an  
121 appropriate amount of a  $1000 \pm 0.5 \text{ mg}\cdot\text{kg}^{-1}$  Y or Rh solution (to reach a final  
122 concentration of  $15 \text{ mg}\cdot\text{kg}^{-1}$ ) was added to 2mL of the target sample or standard for  
123 internal standardization. Afterwards, the resulting solution was thoroughly  
124 homogenized using a Vortex device and an aliquot of  $10\mu\text{L}$  was transferred onto a  
125 quartz glass sample carrier and dried using an infrared lamp ( $T \approx 80\text{-}100^\circ\text{C}$ ) placed  
126 under a laminar flow hood. Subsequently, the sample was analyzed using a  
127 measurement time of 1000s if not otherwise indicated within the manuscript.

### 128 **2.4 Data treatment**

129 The evaluation of TXRF spectra and calculation of the analyte net peak area were  
130 performed using the provided software (Spectra Plus 5.3, Bruker AXS Microanalysis  
131 GmbH, Berlin, Germany). For the peak integration, the software applies a  
132 deconvolution routine which uses measured mono-element profiles for the evaluation  
133 of peak areas. The Fe and Cu concentrations were calculated using the equations in  
134 Table 2. The combined uncertainties indicated are expanded uncertainties  $U = k u_c$   
135 where  $u_c$  is the combined standard uncertainty and  $k$  is a coverage factor equal to 2.  
136 All intermediate steps are standard uncertainties ( $k=1$ ). Combined uncertainties were  
137 obtained by propagating together individual uncertainty components according to the  
138 Guide for Uncertainty in Measurements [19] using the GUM workbench software [20].

139

## 140 **3. Results and discussion**

141

### 142 **3.1 Mathematical description of the measurement procedure**

143 The basic purpose of an uncertainty statement is to propose a range of possible 'true'  
144 values. There are various ways of estimating uncertainties. In the uncertainty  
145 estimation proposed in the GUM, the measurement procedure is described by a  
146 mathematical model and the values and associated standard uncertainties of the  
147 different components in the model must be established [19]. Therefore, a set of  
148 mathematical equations to describe the TXRF measurement processes is given in  
149 Table 2. In the TXRF software, the analyte concentration is calculated using the  
150 intensity ratio between the analyte (A) and the internal standard (IS), the  
151 concentration of the IS ( $C_{IS}$ ) and the sensitivity factor (S) between A and IS. In  
152 equation 1 (Table 2) we also included the dilution factor (DF) arising from the addition  
153 of the IS to the samples, which has a value just above 1. The ratio between A and IS  
154 was calculated using equation 2a. The counts on A and IS are introduced as  
155 constants, not carrying an uncertainty. Instead, two unity multiplicative factors were  
156 introduced to carry standard uncertainties associated with the instrumental  
157 repeatability and depositional repeatability, which are discussed in more detail in  
158 Section 3.2. The software has build-in sensitivity factors. However, to be able to  
159 obtain their uncertainty, in this work the sensitivity factors were determined using a  
160 linear regression (equation 3a, Table 2) using triplicate measurements at 8 different  
161 levels of analytes (Cu and Fe, 25-200  $\text{mg}\cdot\text{kg}^{-1}$ ) with constant level of the internal  
162 standard elements (Y and Rh,  $\approx 100 \text{ mg}\cdot\text{kg}^{-1}$ ). Lastly, the concentration of the IS was  
163 calculated using the concentration of the stock and the masses of respectively the IS solution  
164 and the sample (equation 4b). Additionally, this equation includes a correction for the initial IS  
165 concentration in the sample. Although the internal standard concentrations in the  
166 original sample prior to spiking were below detection limit, the initial concentrations  
167 do carry an uncertainty which was taken into account in the uncertainty budget. The  
168 masses of the IS stock solution and the sample were also used to determine the DF  
169 (equation 4a).

### 171 **3.2 Assessing standard uncertainties**

#### 172 3.2.1 Intensity ratios

##### 173 *3.2.1.1 Instrumental repeatability*

174 In Section 3.1, a unity multiplicative factor carrying the standard uncertainty  
175 associated to the instrumental repeatability was introduced. In order to test the  
176 instrumental repeatability, 10  $\mu\text{L}$  of a standard solution containing  $\approx 2 \text{ mg}\cdot\text{kg}^{-1}$  of Cu,  
177  $\approx 10 \text{ mg}\cdot\text{kg}^{-1}$  of Fe (analytes of interest),  $\approx 10 \text{ mg}\cdot\text{kg}^{-1}$  of Rh and  $\approx 20 \text{ mg}\cdot\text{kg}^{-1}$  of Y  
178 (elements for internal standardization) was analysed for 200, 500, 1000, 1500 and

179 2000 seconds. The same sample on the same reflector was used throughout this  
180 experiment, which was removed and re-introduced into the total-reflection chamber  
181 between each measurement.

182 The Poisson statistic on intensity level was calculated using:

$$183 \quad \sigma = \sqrt{N_X + 2N_{BCK}} \quad (1)$$

184 in which N is the number of counts of respectively element X and its background  
185 (BCK). The standard deviation of the 20 replicates against the average counts for Fe  
186 and Cu is compared with the theoretical value obtained using Poisson statistics  
187 (Figure 1). It can be seen that although the measured standard deviation is much  
188 more scattered, the general trends are similar to those expected based on Poisson  
189 statistics.

190 Since the TXRF procedure uses intensity ratios, a regression between the  
191 experimental standard deviations and the calculated Poisson statistics for the  
192 different analyte/internal standard ratios was performed. A slope of  $0.97 \pm 0.10$  and  
193 an intercept of  $0.0005 \pm 0.0007$  ( $k=1$ ) was obtained. Therefore, we can conclude that  
194 there is no evidence of another contribution for the range of intensities investigated  
195 and that the Poisson distribution can be used to describe the uncertainty on the unity  
196 multiplicative instrumental repeatability.

$$197 \quad u_{inst}(\%) = \sqrt{\frac{\sigma_A^2}{N_A} + \frac{\sigma_{IS}^2}{N_{IS}}} \quad (2)$$

198 The Poisson distribution on intensity level for each element is given in the TXRF  
199 software (sigma values). However, both the analyte and internal standard contribute  
200 to the counting statistics of the ratio (equation 2). This has consequences for the  
201 optimum of internal standard added. Commonly, the internal standard is added at  
202 similar levels as the analyte of interest. In this case, the internal standard contributes  
203 for 50% to the standard uncertainty of the ratio. On the other hand, an internal  
204 standard at much higher levels than the analyte of interest can cause interferences  
205 and loss of sensitivity. Using the Poisson distribution and uncertainty propagation, it  
206 was calculated that having an internal standard intensity 3 times higher than the  
207 intensity of the analyte of interest, the counting statistics of the internal standard  
208 contributes <10 % to the standard uncertainty of the ratio. Therefore, for the  
209 analyses of samples Y and Rh were added at 3 times higher concentrations than the  
210 Fe concentration, the most abundant analyte, to obtain a concentration of  $\approx 15$   
211  $\text{mg} \cdot \text{kg}^{-1}$ .

### 212 3.2.1.2 Depositional repeatability

213 In addition to the instrumental repeatability, small geometric and homogeneity  
214 variations of the deposition on the reflector surface influence the repeatability of the  
215 analyses. In order to test the depositional repeatability and to test if there was an  
216 effect of the sample matrix, different solutions with a concentration of about  $2 \text{ mg}\cdot\text{kg}^{-1}$   
217 of Cu,  $5 \text{ mg}\cdot\text{kg}^{-1}$  Fe and  $15 \text{ mg}\cdot\text{kg}^{-1}$  Rh and Y were deposited on 10 different  
218 reflectors and analysed using 1000 seconds measurement time. The experimental  
219 standard deviations obtained are the combination of the instrumental and the  
220 depositional repeatability. The results in Table 3 show that the signal is strongly  
221 influenced by the deposition. Experimental standard deviations are 4 to 9 times  
222 higher than the theoretical counting statistics. It is often assumed that internal  
223 standardization corrects for such depositional effects [2]. Nevertheless, also using  
224 the ratio (element/internal standard) the experimental standard deviation (between  
225 2.8 and 9.4%) was higher than the Poisson distribution (between 2.4 and 4.0 %).  
226 The depositional repeatability was calculated by subtracting the effect of the  
227 instrumental repeatability from the empirical repeatability based on the standard  
228 deviation:

$$229 \quad u_{dep}(\%) = \sqrt{u_{emp}^2(\%) - u_{instr}^2(\%)} \quad (3)$$

230 It can be observed that the depositional repeatability is high for the mine water and  
231 much lower for the CRM (waste water).

232 In a previous work [10] the variations for multiple measurements were explained by  
233 differences in internal standard concentrations. However, we used different aliquots  
234 of the same spiked solution for the different reflectors. Therefore, the internal  
235 standard concentration is the same for each repeat measurements. Additionally, the  
236 average counts are within uncertainty the same for each solution analyses and can  
237 therefore not explain the differences in the experimental standard deviation. It was  
238 previously observed that a more complex matrix increases the background in the  
239 spectra [2, 21]. Moreover, different reflectors having an altered roughness can  
240 increment the variability of the background associated with the Compton peak [13].  
241 In the samples, the relative background (background/net signal) ranges from 3.6%  
242 for Fe in the tap and river water up to 15% for Cu in the waste water. Nevertheless,  
243 there was no correlation between the spectral background and the experimental  
244 standard deviation. Additionally, no link between the experimental standard deviation  
245 and the presence of certain elements (e.g. Ca, Na) was present. Lastly, the  
246 depositional effects depend on the elemental ratio considered (Table 3). This all



247 indicates that the sample matrix alone cannot explain the depositional repeatability.  
248 Since the controlling factors of the depositional repeatability are not well understood,  
249 it is difficult to come up with one general standard uncertainty value of the unity  
250 multiplicative factor associated to the depositional repeatability.

### 251 *3.2.1.3 Peak deconvolution*

252 The peak deconvolution is performed in an automatic way by the software. In this  
253 work, it is assumed that the uncertainty associated within this process is low and  
254 taken into account by the empirical repeatability. However, in this light it is important  
255 to check for peak overlap. For this reason, Ga was discarded as potential internal  
256 standard from this study since at the concentration levels of interest it overlaps with  
257 the Cu peak (Ga-K $\alpha$ : 9.251 keV, Cu-K $\beta$ :8.907 keV). Usually, the fit quality is tested  
258 using a statistical parameter named Chi,  $\chi$ . This value is calculated as the  
259 standardized square sum of the differences between the measured and the  
260 calculated, deconvoluted intensities for all channels [2]. The value for the fit quality  
261 should preferably be smaller than 10. Higher values are an indication of a poor fit  
262 quality [22]. For our samples, chi values were <4, indicating that no major issues  
263 with peak overlap or peak fitting were present.

### 264 3.2.2 Internal standardization

265 It is assumed that when working under conditions of total reflection, the elemental  
266 intensity ratios measured are directly proportional to the mass fractions of elements  
267 present. Therefore, quantification, can be done by using a single set of relative  
268 sensitivities and a known concentration of an internal standard (see equation 1 in  
269 Table 2). Additionally, as discussed above, internal standardization helps to eliminate  
270 some of the variations caused by effects from deposition on the reflector.

271

272 In this work the sensitivity factors were determined using a linear regression  
273 (equation 3a, Table 2) for different analyte/internal ratios. The standard uncertainties  
274 of the sensitivity factors were obtained using the statistical uncertainty of the  
275 regression between  $N_E$  and  $N_{RF} * C_E * C_{RF}$  using 24 data points (8 levels x 3 replicates),  
276 as for example described in [23, 24]. The resulting standard uncertainties (Table 3)  
277 were between 1.3 and 1.8%.

278

279 Different factors contribute to the uncertainty on the concentration of the IS  
280 (equation 4b, Table 2). Firstly, the addition of the internal standard can be performed  
281 by volume or by weight. When using an analytical balance the contribution of the  
282 weighing error to the total combined uncertainty using our dataset was <0.1%. When

283 volumetric rather than gravimetric dilution data were used, uncertainties of volumes  
284 contribute several percent to the total combined uncertainty. Secondly, any IS  
285 present in the original sample will contribute to the final concentration in the spiked  
286 samples. Therefore, all samples were tested without any addition of IS. As an  
287 example, in Figure 2 TXRF spectra for the certified reference material SPS-WW2  
288 (waste water) with and without addition of Y and Rh as internal standards is  
289 displayed. It was found that for our sample the signal was  $<0.2\%$  than the signal in  
290 the spiked samples. Therefore, the correction for the signal deriving from the original  
291 sample causes  $<0.05\%$  uncertainty on the measured ratio ( $k=1$ ) and is therefore  
292 negligible compared to the effect of other factors. Thirdly, the stated uncertainty ( $5 \text{ mg}\cdot\text{kg}^{-1}$ )  
293 <sup>1)</sup> on the concentration ( $1000 \text{ mg}\cdot\text{kg}^{-1}$ ) of the stock solution has to be taken into account.

294

295 In this study both Y and Rh were used for internal standardization. The results and  
296 uncertainties (see Section 3.2 and Table 4) do not show a systematic difference  
297 between the IS. Both elements were present below TXRF detection limits in our  
298 samples prior to spiking (Figure 2). However, since Y concentration is general more  
299 abundant in natural samples [25], it might be better to use Rh. Yet, the proper choice  
300 of the internal standard should be carried out for each analysed sample.

301

### 302 **3.3 Measurement uncertainty**

303 The uncertainty budget was calculated using the equations and standard  
304 uncertainties as described above and the GUM workbench software for uncertainty  
305 propagation. The total combined uncertainty (coverage factor  $k=2$ , corresponding to  
306 a confidence interval of 95%) was between 6 and 19% (Table 4). The uncertainty  
307 budget for Cu in the municipal waste and mine water samples is illustrated in Figure  
308 3. For all samples and both analytes, the ratio repeatability (assessed by measuring  
309 the same solution deposited at different reflectors) is the main contributor to the  
310 uncertainty budgets. However, the relative contribution of the instrumental and  
311 depositional varies. For example, for the SPS-WW2 the main contributor is the  
312 instrumental repeatability, while for the mine water the depositional repeatability is  
313 the main contribution (Figure 3). The sensitivity factor contributes up to 20% to the  
314 combined expanded uncertainty. The concentration of the IS present in the sample  
315 (i.e. weighing, concentration of the stock and the original IS concentration in the  
316 samples) seems only a minor contribution to the total combined uncertainty for our  
317 measurements.

318

319 The provided sigma-concentration by the TXRF software, which is based on the  
320 counting statistics of the analyte, is much lower compared to the combined expanded  
321 uncertainty, since the counting statistics of the analyte just contribute between 23-  
322 70% to the total combined uncertainty. Moreover, in the case the internal standard  
323 has similar counts to the analyte, the software will further underestimate the  
324 uncertainty by at least a factor of 2. This could be one of the reasons why  
325 intercomparison studies lead to statistically different results [9]. It would be  
326 beneficial if TXRF software could take the effect of the counting statistics of the  
327 internal standard and the uncertainty of the sensitivity factor into account. However,  
328 at present it will be a major challenge to include the depositional repeatability in the  
329 software, since it varies from sample to sample and it is unclear which factors  
330 influence this uncertainty.

331

332 Therefore, an alternative approach was tested for the waste and mine water sample  
333 in which the empirical standard uncertainty of the repeatability (which includes both  
334 the instrumental and depositional repeatability) was calculated based on 3  
335 measurements on 3 different reflectors. The uncertainty budgets using Rh as an  
336 internal standard are given in Figure 4. It can be observed that the concentrations  
337 results are the same within uncertainty as the previous uncertainty budget. However,  
338 uncertainties are lower since the repeatability was divided by the square root of the  
339 number of independent measurements. Additionally, the contribution of the  
340 sensitivity factor does increase following this approach. This approach allows the  
341 estimation of the uncertainty without understanding the depositional repeatability.  
342 Nevertheless, as this depositional repeatability is 9-68% of the total combined  
343 uncertainty, future research on the factors influencing the depositional repeatability  
344 and ways how to lower this uncertainty would be a major step forward in improving  
345 the uncertainty for TXRF analyses.

346

### 347 **3.4 Accuracy of TXRF**

348 The obtained values using TXRF could be compared with ICP-OES analyses and  
349 reference or calculated values, the latter based on the amount of spike added (Table  
350 4). In general there is no evidence for bias since TXRF and ICP-OES or  
351 reference/calculated values and are the same at a 95% confidence interval. However,  
352 for the spiked tap water, the Cu content is higher than the theoretical value. Given  
353 the good results for the other samples, we believe this is related to presence of Cu  
354 in the non-spiked matrix. In summary, there is no evidence that one of the main  
355 factors influencing the uncertainty was not taken into account in this study.

356 **3.5 Practical approach to obtain the measurement uncertainty**

357 A detailed evaluation of the uncertainty budget, showed that 2 or 3 parameters form  
358 >95% of the uncertainty budget. Therefore, the relative combined expanded  
359 uncertainty ( $U_{Ca}(\%)$ ), can be approximated by combining the uncertainty of the  
360 instrumental repeatability ( $u_{inst}$ ), the deposition ( $u_{dep}$ ) and the sensitivity factor ( $u_s$ ),  
361 using a simple set of equations:

362 
$$U_{CA}(\%) \approx 2 \cdot \sqrt{u_{inst}^2 + u_{dep}^2 + u_s^2} = 2 \cdot \sqrt{u_{emp}^2 + u_s^2} \quad (4)$$

363 As discussed above the standard uncertainty on the instrumental repeatability can  
364 be described using the Poisson distribution (equation 2). This are all parameters  
365 which can be easily deducted from the software. The standard uncertainty on the  
366 depositional repeatability can be determined using the difference between the  
367 empirical repeatability (standard deviation of replicate measurements) and the  
368 instrumental repeatability (equation 3). Alternatively, the instrumental and  
369 depositional repeatability can be taken together if the multiple measurements were  
370 performed for one sample on different reflectors. In this case, the standard empirical  
371 uncertainty of the repeatability ( $u_{emp}$ ) can be determined by the standard deviation  
372 divided by the square root of the number of replicates ( $n$ ).

373 For the uncertainty on the sensitivity factor ( $u_s$ ), a regression between the analyte  
374 and the internal standard should be performed. In principle, this only needs to be  
375 performed once for each TXRF system. General statistics can then be used to  
376 determine the slope and its relative uncertainty.

377 It is important to realize that this approximation of the uncertainty budget is only  
378 valid if the concentration of the internal standard does not significantly contribute to  
379 the uncertainty budget. This means that the internal standard additions should be  
380 performed by weight by a calibrated balance, that the presence of the IS in the non-  
381 spiked sample should be checked and that the concentration of the IS stock solution  
382 should have a low uncertainty. Although this is not a complete uncertainty budget,  
383 this practical approach provides a more realistic uncertainty estimate compared to  
384 the sigma value of the analyte provided by most softwares.

385 **4. Conclusion**

386 The parameters contributing to the measurement of uncertainty are summarized in  
387 Figure 5. The instrument variability seems to be mainly controlled by counting  
388 statistics for studied range (up to 5000 counts). In order to avoid that the counting

389 statistics of the internal standard significantly contribute to the total combined  
390 uncertainty, it is recommended that the concentration of the internal standard is  
391 about 3 times higher than the analytes of interest. Nevertheless, the empirical  
392 repeatability of the ratio is higher than the Poisson distribution. Although it is  
393 generally believed that depositional effects can be eliminated by normalisation to an  
394 internal standard, in this study it is shown that the ratio repeatability using different  
395 reflectors is higher than expected based on Poisson statistics. The factors influencing  
396 this depositional repeatability could not be determined. In order to get a realistic  
397 uncertainty budget with one replicate, future work should try to determine the  
398 controlling factors of the ratio repeatability. Moreover, since the depositional  
399 repeatability is a main contribution to the uncertainty budget, a mechanistic  
400 understanding of the depositional effects could potentially be used to decrease the  
401 uncertainty associated to TXRF measurements. By a lack of theoretical prediction of  
402 the depositional repeatability, the uncertainty budget can be based on replicate  
403 measurements (using different reflectors). Another important contribution to the  
404 uncertainty is the sensitivity factor, which contributes up to 50%. Currently, most  
405 software provides the sigma-concentration, which reflects the influence of the  
406 counting statistics of the analyte on uncertainty. However, this is not a good  
407 representation of the total combined uncertainty. Therefore, we provided a simple  
408 approach to obtain a more realistic uncertainty budget.

409

#### 410 **Acknowledgments**

411 This work has been funded by the Spanish National Research Programme (CGL-  
412 2010-22168-C03-01).

413

414

415 **References**

416

417 [1] C.Streli, Recent advances in TXRF, *Appl. Spectrosc. Rev.* 41 (2006) 473-489.

418

419 [2] R. Klochenkämper, Total reflection X-ray fluorescence analysis, vol. 140 in *Chemical*  
420 *Analysis: A Series of Monographs on Analytical Chemistry and its Applications*, John Wiley &  
421 Sons, New York, 1997.

422 [3] E.Marguí, R.Van Grieken, *X-ray fluorescence spectrometry and related techniques: An*  
423 *introduction*, Momentum Press, New York, 2013.

424 [4] E.Marguí, J.C.Tapias, A.Casas, M.Hidalgo, I.Queralt, Analysis of inlet and outlet industrial  
425 wastewater effluents by means of benchtop total reflection X-ray fluorescence spectrometry,  
426 *Chemosphere* 80 (2010) 263-270.

427 [5] E.Marguí, I.Queralt, M.Hidalgo, Determination of platinum group metal catalyst residues in  
428 active pharmaceutical ingredients by means of total reflection X-ray spectrometry,  
429 *Spectrochim. Acta B* 86 (2013) 50-54.

430 [6] S.Kunimura, D.Watanabe, J.Kawai. Optimization of a glancing angle for simultaneous trace  
431 elemental analysis by using a portable total reflection X-ray fluorescence spectrometer.  
432 *Spectrochimica Acta Part B* 64 (2009) 288-290.

433 [7] P. Deines, S.L. Goldstein, E.H. Oelkers, R.L. Rudnick, L.M. Walter. Standards for  
434 publication of isotope ratio and chemical data in *Chemical Geology*, *Chemical Geology* 202  
435 (2003) 1-4.

436

437 [8] H. Egli, M. Dassenakis, H. Garelick, R. van Grieken, W. J. G. M. Peijnenburg, L. Klasinc, W.  
438 Kördel, N. Priest, T. Tavares. Minimum requirements for reporting analytical data for  
439 environmental samples (IUPAC Technical Report). *Pure and Applied Chemistry* 75 (2009): 999-  
440 1155

441

442 [9] P.J. Potts, Proposal for the Publication of Geochemical Data in the Scientific Literature.  
443 *Geostandards and Geoanalytical Research* 36 (2012) 225-230

444

445 [10] L. Borgese, F. Bilo, K. Tsuji, R. Fernández-Ruiz, E. Margui, C. Streli, G. Pepponi, H.  
446 Stosnach, T. Yamada, P. Vandenberghe, D.M. Maina, M. Gatari, K.D. Shepherd, E.K. Towett,  
447 L. Bennun, G. Custo, C. Vasquez, L.E. Depero. First Total Reflection X-Ray Fluorescence round-  
448 robin test of water samples: Preliminary results, *Spectrochimica Acta Part B: Atomic*  
449 *Spectroscopy* 101 (2014): 6-14

450

451 [11] ISO/IEC, General requirements for the competence of testing and calibration laboratories,  
452 ISO/IEC 17025:2005, International Organization for Standardization/International  
453 Electrotechnical Commission, Geneva, 2005.

454 [12] O.K. Owoade, F.S. Olise, H.B. Olaniyi, D. Wegrzynek. Model estimated uncertainties in  
455 the calibration of a total reflection x-ray fluorescence spectrometer using single-element  
456 standards. *X-Ray Spectrometry* 35 (2006) 249-252.

457 [13] R. Fernández-Ruiz. Uncertainty in the multielemental quantification by total-reflection X-  
458 ray fluorescence: theoretical and empirical approximation. *Analytical chemistry* 80.22 (2008):  
459 8372-8381.

460 [14] B.P. Zietz, H.H. Dieter, M. Lakomek, H. Schneider, B. Keßler-Gaedtke, B., H. Dunkelberg.  
461 Epidemiological investigation on chronic copper toxicity to children exposed via the public  
462 drinking water supply. *Science of the total environment* 302 (2003), 127-144.

463 [15] T. Theophanides, J. Anastassopoulou, Copper and carcinogenesis, *Critical Reviews in*  
464 *Oncology/Hematology* 42 (2002): 57-64,

465

466 [16] Directive 2000/60/EC of the European Parliament and of the Council of 23  
467 October 2000 establishing a framework for Community action in the field of water  
468 policy, Official Journal of the European Communities L 327/1, 22/12/2000.

469 [17] T. D. Jickells, Z. S. An, K. K. Andersen, A. R. Baker, G. Bergametti, N. Brooks, J. J. Cao, P.  
470 W. Boyd, R. A. Duce, K. A. Hunter, H. Kawahata, N. Kubilay, J. laRoche, P. S. Liss, N.  
471 Mahowald, J. M. Prospero, A. J. Ridgwell, I. Tegen, R. Torres. Global Iron Connections between  
472 desert dust, ocean biogeochemistry and climate. *Science* 308 (2005): 67-71.

473 [18] A.B. Cundy, L. Hopkinson, R.L.D. Whitby. Use of iron-based technologies in contaminated  
474 land and groundwater remediation: A review. *Science of The Total Environment* 400 (2008)42-  
475 51  
476

477 [19] JCGM 100, Evaluation of measurement data — Guide to the expression of uncertainty in  
478 measurement; Joint Committee for Guides in Metrology (BIPM, IEC, IFCC, ISO, IUPAC, IUPAP,  
479 OIML, ILAC), BIPM, [www.bipm.org](http://www.bipm.org), Paris, 2008.

480 [20] Metrodata GmbH, 2003. Gum Workbench. The software tool for the expression of  
481 uncertainty in measurement. Metrodata GmbH, D-79639 Grenzach-Wyhlen, Germany.

482 [21] E. Marguí, G. H. Floor, M. Hidalgo, P. Kregsamer, G. Román-Ross, C. Strelí and I. Queralt.  
483 Applicability of direct total reflection X-ray fluorescence analysis for selenium determination in  
484 solutions related to environmental and geochemical studies. *Spectrochimica Acta B* 25 (2010):  
485 1002-1007

486 [22] S2 PICOFOX™ User Manual. Bruker advanced X-ray solutions. Bruker AXS Microanalysis  
487 GmH, Berlin (Germany), 2007.

488 [23] Miller, J.N., 1991. Basic statistical methods for analytical chemistry. Part 2. Calibration  
489 and regression methods. A review. *Analyst* 116: 3-14.

490 [24] Press, W.H., 2012. *Numerical Recipes in C: The Art of Scientific Computing*.

491 [25] K. Hans Wedepohl. The composition of the continental crust. *Geochimica et cosmochimica*  
492 *Acta* 59 (1995) 1217-1232.

493 [26] <http://www.lgcstandards.com/CA/en/Waste-water-Trace-metals/p/SPS-WW2>. Accessed  
494 16-06-2015.  
495  
496  
497

498 **Table 1.**

499 Instrumental parameters and measurement conditions

---

<b>S2 PICOFOX TXRF benchtop spectrometer</b>	
X-Ray tube	W
Rating	50 kV, 1mA (maximum power 50 W)
Optics	Multilayer monochromator (33.0 keV)
Detector	Si drift detector, 10mm <sup>2</sup> , <160eV resolution Mn-K <sub>α</sub>
Working environment	Air
Sample station	Cassette changer for 25 samples
Size, weight	600x300x450mm, 37kg
Measurement time	1000 s
Analytical lines	Cu, Fe, Y, Rh: K-lines

---

<b>Varian Liberty RL ICP-OES spectrometer</b>	
Element wavelength	Fe:238.204nm, Cu:324.754nm
RF power	1000 W
Plasma gas flow rate	12 L min <sup>-1</sup>
Auxiliary gas flow rate	1.5 L min <sup>-1</sup>
Nebulizer	V-groove

---

500

501



**Table 2: mathematical model of the measurement procedure**

<b>Key equation</b>	
Concentration of the analyte using internal standardization	
1: $C_A = R \cdot \frac{C_{IS} \cdot DF}{S}$	
<b>Intensity ratio</b>	
Ratio between analyte and internal standard (1 measurement):	
2a: $R = \frac{N_A}{N_{IS}} \cdot \delta_{inst} \cdot \delta_{dep}$	
Unity multiplicative factor arising with instrumental repeatability:	
2b: $\delta_{inst} = 1$	
Unity multiplicative factor arising with depositional repeatability:	
2c: $\delta_{dep} = 1$	
<b>Sensitivity factor</b>	
Least Square regression of $N_E$ versus $N_{RF} \cdot C_E \cdot C_{RF}$ :	
3a: $S = \frac{n \cdot \sum \left[ N_{RF\_i} \cdot \frac{C_{E\_i}}{C_{RF\_i}} \cdot N_{E\_i} \right] - \sum \left[ N_{RF\_i} \cdot \frac{C_{E\_i}}{C_{RF\_i}} \right] \cdot \sum N_{E\_i}}{n \cdot \sum \left[ N_{RF\_i} \cdot \frac{C_{E\_i}}{C_{RF\_i}} \right]^2 - \left( \sum N_{RF\_i} \cdot \frac{C_{E\_i}}{C_{RF\_i}} \right)^2}$	
<b>Concentration internal standard</b>	
Dilution factor of the solution	
4a: $DF = \left( \frac{m_{smp} + m_{IS}}{m_{smp}} \right)$	
Concentration of the IS	
4b: $C_{IS} = C_{Stock} \frac{m_{IS}}{m_{smp}} + C_0$	

Parameter	Index
C	Concentration (mg·kg <sup>-1</sup> )
A	Analyte of interest (in sample)
N	Intensity (counts)
IS	Internal standard (in sample)
R	Intensity ratio
E	Element of interest (for determination of sensitivity, same element as A)
S	Sensitivity factor
RF	Reference element (for determination of sensitivity, same element as IS)
m	Mass (in kg)
smp	sample
DF	Dilution factor
stock	Stock solution
δ	Multiplicative unity factors
0	Sample without spike
x,i	Generic indices

**Table 3: input parameters for the set of equations of Table 2. An uncertainty of 0.2 mg was taken for the weighing, the uncertainty of the stock solution of the internal standards was 5 mg·kg<sup>-1</sup> (k=1).**

Sample	Parameter		Signal		Ratio				Sample prep; weight in g		
			Fe	Cu	Fe/Y	Fe/Rh	Cu/Y	Cu/Rh	m <sub>sample</sub>	m <sub>Y</sub>	m <sub>Rh</sub>
	Sensitivity factor	Value			0.267	0.318	0.446	0.531			
		u(k=1)			0.004	0.005	0.006	0.010			
CRM SPS-WW2	Intensity		1513	1022	0.081	0.096	0.055	0.065	2.964	0.046	0.046
	Empirical rep. (%)		25.6	26	2.8	4.5	2.7	3.5			
	Instrumental rep. (%)		2.8	3.5	2.7	2.7	3.3	3.3			
	Depositional rep. (%)		25.4	25.8	0.7	3.6	<0	1.2			
Spiked tap water	Intensity		1618	1377	0.078	0.093	0.065	0.079	3.112	0.046	0.044
	Empirical rep. (%)		20.5	18.6	7.4	6.9	4.4	3.8			
	Instrumental rep. (%)		2.8	3.1	2.4	2.4	2.6	2.6			
	Depositional rep. (%)		20.3	18.3	7.0	6.5	3.5	2.8			
Spiked river Water	Intensity		1589	1197	0.080	0.092	0.060	0.069	3.059	0.045	0.046
	Empirical rep. (%)		12.5	12.4	4.7	4.5	5.2	5.2			
	Instrumental rep. (%)		2.8	3.3	2.6	2.6	2.9	3.0			
	Depositional rep. (%)		12.2	12.0	3.9	3.7	4.3	4.2			
Waste water	Intensity		1555	1201	0.070	0.082	0.054	0.063	15.65	0.235	0.236
	Empirical rep. (%)		13	12.7	4.9	4.5	4.2	4.4			
	Instrumental rep. (%)		2.4	2.9	3.2	3.3	3.9	4.0			
	Depositional rep. (%)		12.8	12.4	3.7	3.1	1.6	1.8			
Mine water	Intensity		1600	1271	0.076	0.087	0.061	0.069	15.12	0.233	0.235
	Empirical rep. (%)		10.3	11.7	9.4	9.1	7.6	6.4			
	Instrumental rep. (%)		2.7	3.1	2.6	2.9	2.9	3.2			
	Depositional rep. (%)		9.9	11.3	9.0	8.6	7.0	5.5			

**Table 4.** TXRF results for the analysis of different types of water samples. Concentrations ( $\text{mg}\cdot\text{kg}^{-1}$ ) obtained by ICP-OES and theoretical values (added amount of analyte to the sample matrix or consensus values)<sup>26</sup> are given for comparison.

	Analyte	TXRF						ICP-OES	References/ Calculated
		IS=Rh			IS=Y				
		Value	U (k=2)		Value	U (k=2)			
CRM SPS-WW2	Cu	1.96	0.16	8.2%	1.96	0.14	7.1%	1.9±0.1	2.0±0.01
	Fe	4.85	0.47	9.7%	4.70	0.30	6.4%	4.8±0.3	5.0±0.025
Spiked tap water	Cu	2.18	0.19	8.7%	2.23	0.21	9.4%	-	1.87
	Fe	4.31	0.61	14.2%	4.26	0.64	15.0%	-	4.53
Spiked river water	Cu	2.03	0.22	10.8%	2.06	0.22	10.7%	-	1.90
	Fe	4.49	0.43	9.6%	4.42	0.44	10.0%	-	4.58
Waste water	Cu	1.91	0.18	9.4%	1.91	0.17	8.9%	1.8±0.1	-
	Fe	4.13	0.40	9.7%	4.01	0.41	10.2%	4.3±0.2	-
Mine water	Cu	2.16	0.29	13.4%	2.23	0.34	15.2%	2.0±0.1	-
	Fe	4.55	0.84	18.5%	4.54	0.86	18.9%	4.7±0.2	-

## FIGURE CAPTIONS

**Figure 1.** Comparison of measured standard deviation based on 20 replicate measurements of the same reflector ( $\text{Cu} \approx 2 \text{ mg}\cdot\text{kg}^{-1}$  and  $\text{Fe} \approx 10 \text{ mg}\cdot\text{kg}^{-1}$ ) and Poisson statistics.

**Figure 2.** TXRF spectra for the certified reference material SPS-WW2 (Waste water, 2 and 5  $\text{mg kg}^{-1}$  of Cu and Fe) with and without addition of Y and Rh as internal standards ( $15 \text{ mg kg}^{-1}$ ).

**Figure 3.** Relative contributions to the Cu uncertainty budget using the instrumental and depositional repeatability and Rh as internal standard the waste and mine water sample.

**Figure 4.** Relative contributions to the Cu and Fe uncertainty budget using the empirical repeatability and Rh as internal standard for the waste water and mine water sample.

**Figure 5.** Ishikawa diagram for the TXRF measurement procedure.

**Figure 1**

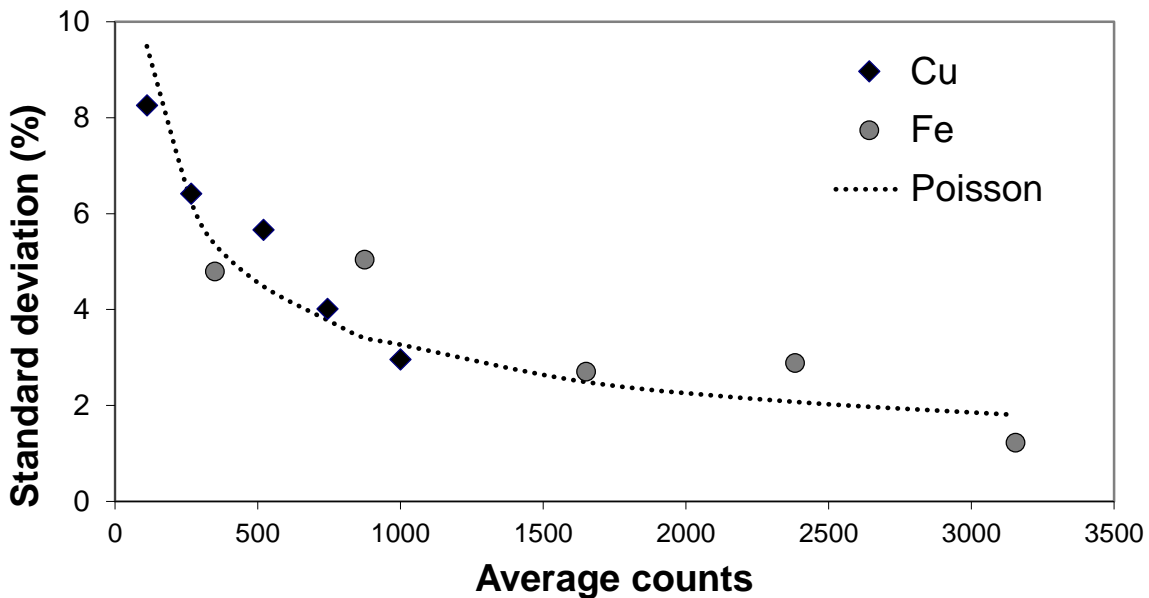
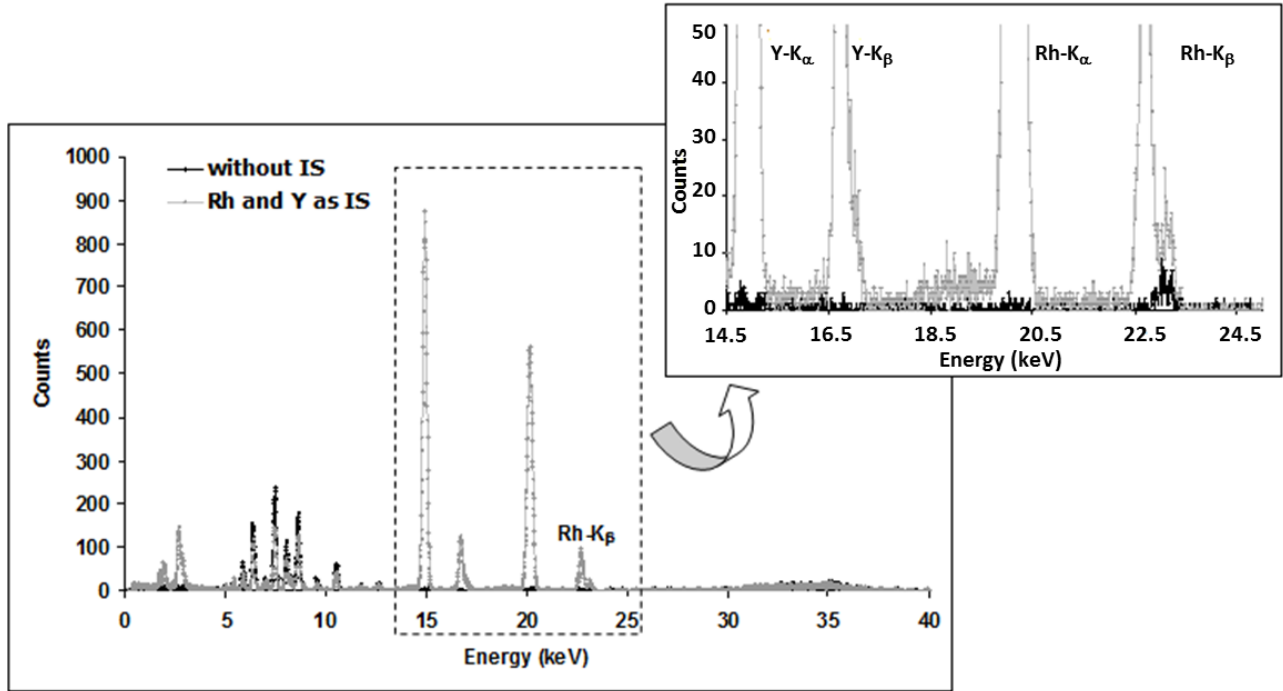
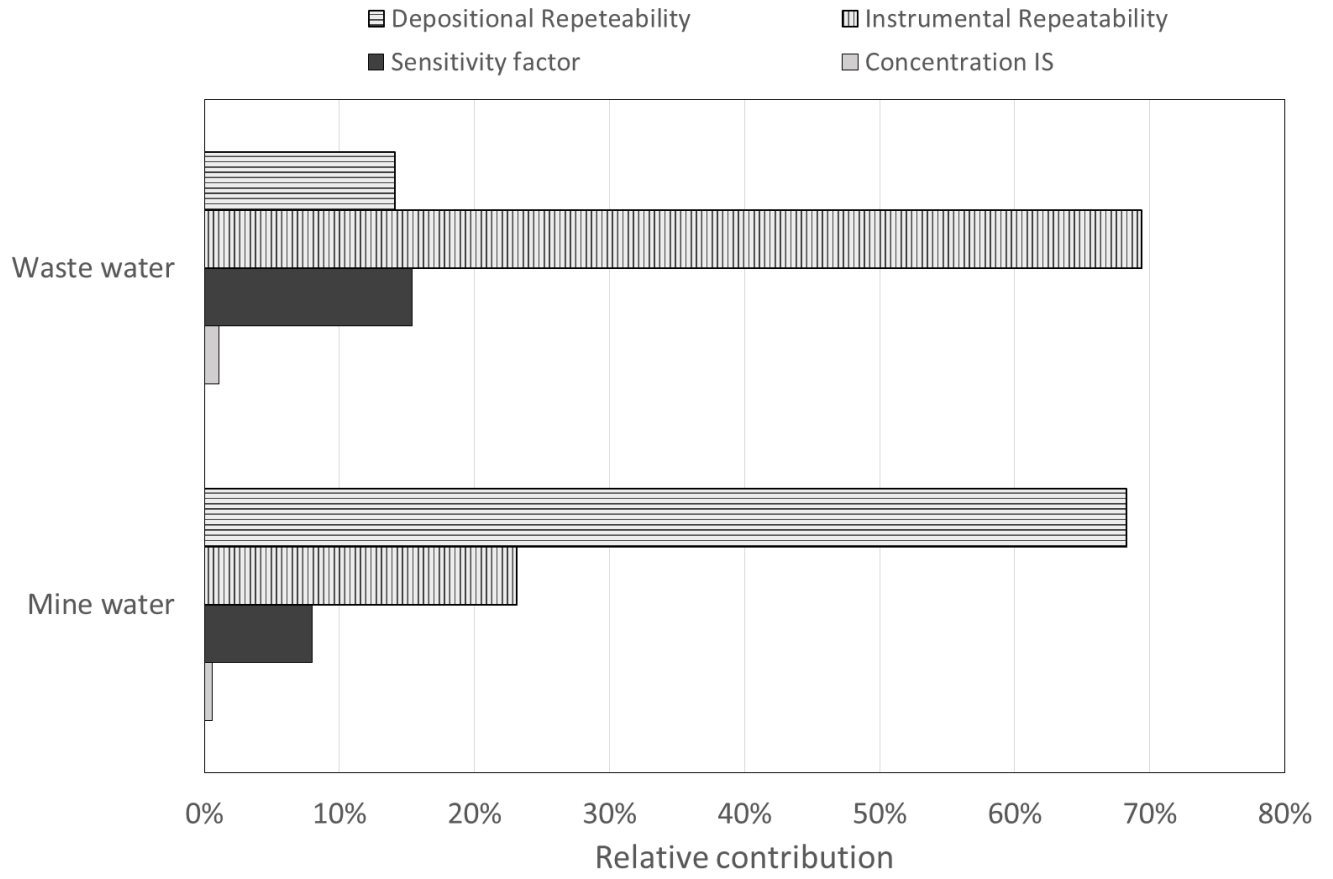


Figure 2



**Figure 3**



**Figure 4**

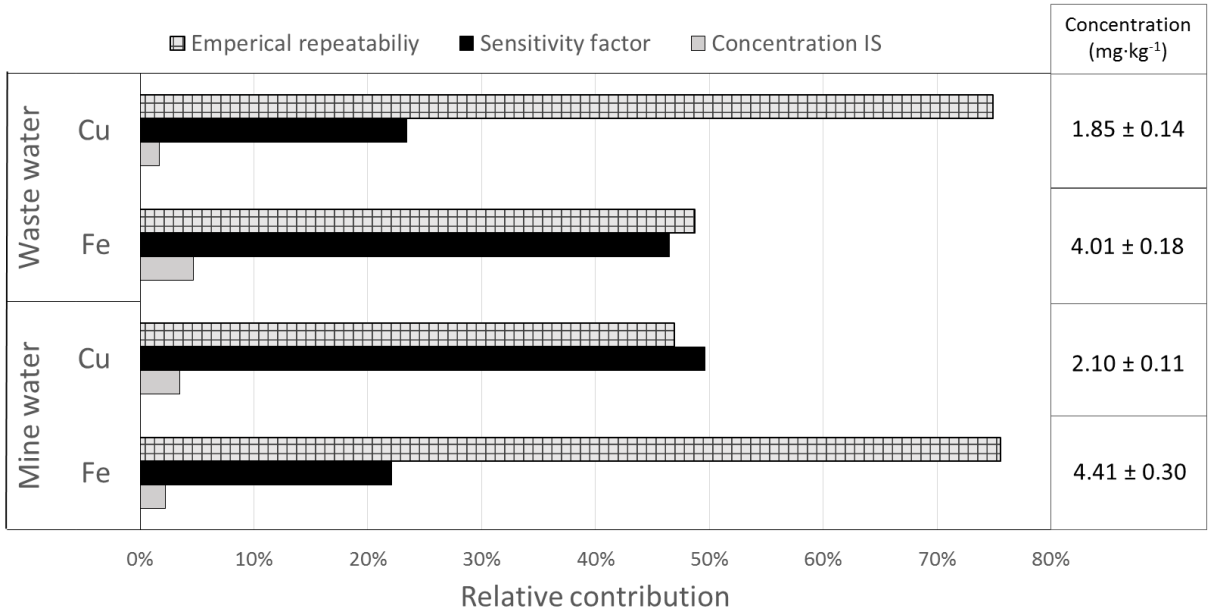


**Figure 5**

